Journal of Power Sources 191 (2009) 575–581

Contents lists available at ScienceDirect

Journal of Power Sources

journal homepage: www.elsevier.com/locate/jpowsour

# Thermal stability of $LiPF_6$-based electrolyte and effect of contact with various delithiated cathodes of Li-ion batteries

H.F. Xiang[a,b], H. Wang[a], C.H. Chen[a,*], X.W. Ge[b], S. Guo[c], J.H. Sun[c], W.Q. Hu[a]

[a] Academia Sinica Key Laboratory of Materials for Energy Conversion, Department of Materials Science and Engineering, University of Science and Technology of China, Anhui, Hefei 230026, PR China
[b] Department of Polymer Science and Engineering, University of Science and Technology of China, Anhui, Hefei 230026, PR China
[c] State Key Laboratory of Fire Science, University of Science and Technology of China, Anhui, Hefei 230026, PR China

ARTICLE INFO

*Article history:*
Received 4 August 2008
Received in revised form 16 February 2009
Accepted 17 February 2009
Available online 3 March 2009

*Keywords:*
Lithium-ion batteries
Thermal stability
Electrolyte
Cathode
Safety

ABSTRACT

Thermal stability of $LiPF_6$-based electrolyte (1 M $LiPF_6$/EC + DMC) was studied by in-situ FTIR spectroscopy and C80 calorimetry, which indicated that the electrolyte underwent furious polymerization and decomposition reactions and sharp heat flow was generated below 225 °C. The thermal stability of the electrolyte in contact with various delithiated cathodes ($Li_xCoO_2$, $Li_xNi_{0.8}Co_{0.15}Al_{0.05}O_2$, $Li_xNi_{1/3}Co_{1/3}Mn_{1/3}O_2$, $Li_xMn_2O_4$, $Li_xNi_{0.5}Mn_{0.5}O_2$, $Li_xNi_{0.5}Mn_{1.5}O_4$ and $Li_xFePO_4$) was also investigated by C80 calorimetry. The results show that the cathode materials except for $Li_xFePO_4$ usually have an enhancement effect on the decomposition of the electrolyte, but $Li_xFePO_4$ exhibits a suppression effect on the reactions of the electrolyte. $Li_xFePO_4$ is found to be with excellent thermal stability. Among the other cathodes, $Li_xCoO_2$, $Li_xNi_{0.8}Co_{0.15}Al_{0.05}O_2$, $Li_xNi_{0.5}Mn_{0.5}O_2$ and $Li_xNi_{0.5}Mn_{1.5}O_4$ promote the decomposition of electrolyte by releasing oxygen and thus considered not favorable for safety, but $Li_xNi_{1/3}Co_{1/3}Mn_{1/3}O_2$ with a lesser reaction heat and $Li_xMn_2O_4$ with even less heat flow in the low temperature range (50–225 °C) are believed as promising cathodes for better safety. By comparing X-ray diffraction (XRD) patterns of these cathode materials at room temperature and those heated to 300 °C in the presence of the electrolyte, we have found that $Li_xFePO_4$ only has experienced tiny structure change, which is greatly different from the other cathode materials.



## 1. Introduction

Lithium-ion batteries are now widely used in portable 3C (computer, communication, consumer electronics) products owing to their high energy density. Large-sized lithium-ion batteries and battery packs are also very attractive for electric vehicles (EV), hybrid electric vehicle (HEV) and plug-in hybrid electric vehicle (PHEV) applications. However, safety concern has become one of the most important issues for the development of lithium-ion batteries, because under some abusive conditions, catastrophic reactions between active electrodes and electrolyte result in thermal runaway that drives the flammable electrolyte into fire or explosion. Much effort has been devoted to alleviate the safety issue. Highly safe electrolyte systems such as nonflammable electrolytes [1–8] and ionic liquid electrolytes [9–15] are the direct solutions of this pressing issue. However, some obstacles seem to be inevitable. For example, most nonflammable electrolytes and ionic liquid electrolytes are either incompatible with electrode materials or too expensive to be accepted. Thus, the priority consideration should be to prevent the appearance of thermal runaway.

The thermal runaway of Li-ion batteries usually appears when heat output of battery system exceeds thermal dissipation. Under some abusive conditions, exothermic reactions take place among the flammable electrolyte, highly oxidative cathode material and reductive anode material, and the heat generation further accelerates more exothermic reactions which may eventually result in the thermal runaway. Usually the thermal stability of electrolyte and exothermic reactions between electrolyte and cathode material at elevated temperature are considered as the main contributors to the thermal runaway [16]. The thermal stability of electrolyte has been widely studied by calorimetry and spectroscopy. Yamaki [17] studied the thermal behavior of various electrolyte systems by differential scanning calorimetry (DSC), and Lucht [18] investigated the reaction mechanism of electrolyte at elevated temperature (85–100 °C) by nuclear magnetic resonance (NMR) spectroscopy and gas chromatography with mass selective detection (GC–MS). However, the exothermic reactions related to those exothermic processes in the calorimetric studies are still unclear and ambiguous. It is mostly necessary to decipher the exothermic reaction mechanism of electrolyte using some on-line measurements, which has

* Corresponding author. Tel.: +86 551 3606971 fax: +86 5513602940.
*E-mail address:* cchchen@ustc.edu.cn (C.H. Chen).

0378-7753/$ – see front matter © 2009 Elsevier B.V. All rights reserved.
doi:10.1016/j.jpowsour.2009.02.045

important significance for exploring novel electrolytes for the next generation of Li-ion batteries.

In literature, the thermal stability of electrolyte against lithiated cathodes has been usually studied by DSC and accelerating rate calorimetry (ARC) [19–25]. But the sensitivities of DSC and ARC are not high enough to evaluate the thermal hazards for complex reactive substance in the lower temperature range, i.e. from room temperature to 300 °C, especially for confirming the onset temperature, which is a significant index for evaluating thermal stability. Using the C80 calorimeter with high sensitivity, however, the reaction can easily be detected in the lower temperature range and the identified onset temperature is more accurate than those obtained by DSC and ARC [26]. Recently various cathode materials have widely been studied in academic and industrial laboratories, and also researchers are ceaselessly engaged in the search for new materials for Li-ion batteries. Although the thermal stability of most cathodes has been reported [23–25], the results from different groups, even using different measurements, such as DSC or ARC, cannot be used for an objective comparison with each other. So it is necessary to evaluate thermal stability of various cathode materials in commercial electrolyte for finding suitable materials or guiding new material design in order to improve the safety characteristic of Li-ion batteries.

In-situ Fourier transform infrared spectrometer (FTIR) is an efficient measurement for illuminating thermal reaction mechanism of polymer materials [27,28], herein we also believe that it is a promising measurement for investigating thermal stability of electrolyte of Li-ion batteries. In this paper, thermal stability of commercial $LiPF_6$-based electrolyte is first investigated by in-situ FTIR along with C80 calorimetry, and then the exothermic reaction mechanism is presumed. Based on the results of thermal stability of the electrolyte, effect of seven delithiated cathode materials those have been paid much attention to in the Li-ion battery industry, $Li_xCoO_2$ (LCO), $Li_xNi_{0.8}Co_{0.15}Al_{0.05}O_2$ (Gen2), $Li_xNi_{1/3}Co_{1/3}Mn_{1/3}O_2$ (L333), $Li_xMn_2O_4$ (LMO), $Li_xNi_{0.5}Mn_{0.5}O_2$ (LNMO), $Li_xNi_{0.5}Mn_{1.5}O_4$ (LNM3O) and $Li_xFePO_4$ (LFPO), is compared on the thermal stability of the $LiPF_6$-based electrolyte by C80 calorimetry under the same conditions, in order to direct the research of new cathode materials and design highly safe Li-ion batteries.

## 2. Experimental

1 M $LiPF_6$/ethylene carbonate (EC) + dimethyl carbonate (DMC) (1:1, w/w) was commercially available products made by Zhangjiagang Guotai-Huarong Co., Ltd. Except $LiNi_{0.5}Mn_{1.5}O_4$, other cathode materials were all obtained from commercial products. $LiCoO_2$, $LiMn_2O_4$, $LiNi_{1/3}Co_{1/3}Mn_{1/3}O_2$, $LiNi_{0.5}Mn_{0.5}O_2$ and $LiFePO_4$ were purchased from several Chinese corporations, and $LiNi_{0.8}Co_{0.15}Al_{0.05}O_2$ was supplied by Argonne National Laboratory. $LiNi_{0.5}Mn_{1.5}O_4$ was prepared by a radiated polymer gel (RPG) method, and more details were described elsewhere [29,30]. Composite electrodes consisting of cathode powder (84 wt.%), acetylene black (8 wt.%) and poly(vinylidene fluoride) (PVDF) (8 wt.%) were made by a tape-casting process on aluminum foils. CR2032 coin cells with Li foil anode were assembled in an argon-filled glove box (MBraun Labmaster 130) and then cycled twice on a multichannel battery cycler (Neware BTS2300, Shenzhen) at a current of 0.2 mA $cm^{-2}$, followed by charged to some upper cut-off voltage, especially 4.2 V for LCO and LFPO, 4.3 V for LMO, 4.5 V for Gen2, L333 and LNMO, 5.0 V for LNM3O. All charged cells were then transferred into the glove box for the C80 sample preparation. After the cell disassembly, the positive electrode was taken out and rinsed with DMC to remove the original electrolyte from the surface of electrode, then dried to remove DMC before the cathode materials (containing acetylene black and PVDF) were scraped from the Al current collector. 23 mg cathode material and 50 mg electrolyte of 1 M $LiPF_6$/EC + DMC were added into a stainless sample tube, and then the samples were sealed for the calorimetry measurement by a Setaram C80 calorimeter (Calvet). All the procedure was operated in the glove box to make sure the argon circumstance. The calorimetry measurements were carried out at a heating rate of 0.2 °C $min^{-1}$ from room temperature to 300 °C, and the C80 calculations were based on the weight of the electrolyte.

In-situ FTIR spectra were recorded using a Bruker Vector-22 IR spectrophotometer equipped with a high temperature cell (HTC-3) controlled by an automatic temperature controller (Harrick Scientific Products, Inc.). Electrolyte was dripped into a homemade KBr sample cell in the glove box, and then the sample cell was taken out from the glove box and placed into the HTC-3 cell. The temperature of the cell was raised at a heating rate of about 2 °C $min^{-1}$. Dynamic FTIR spectra were recorded on line during the thermal reaction of electrolyte with the temperature rising.

The crystalline structure of the delithiated cathode was characterized by X-ray diffraction (XRD) using a diffractometer (Philips X'Pert Pro Super, Cu Kα radiation). Followed by opening the charged cells and taking the electrodes out, some electrode laminates were measured directly without further treatment, but others were added with a little electrolyte and then heated to 300 °C in an argon-filled sealed container. The diffraction patterns were recorded at room temperature in the $2\theta$ range from 10° to 80°.

## 3. Results and discussion

The in-situ FTIR spectra of the electrolyte of 1 M $LiPF_6$/EC + DMC heated to different temperatures are shown in Fig. 1a. The signals in the range of 2750–3300 $cm^{-1}$ correspond to the stretching mode

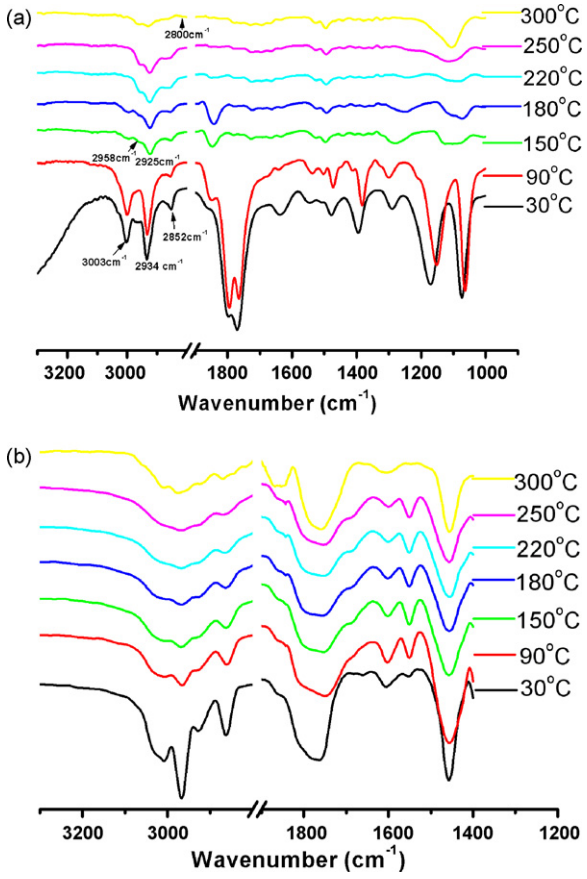


**Fig. 1.** In-situ FTIR spectra of (a) the $LiPF_6$ electrolyte of 1 M $LiPF_6$/EC + DMC (1:1) and (b) the solvents of EC + DMC (1:1) heated to different temperatures.

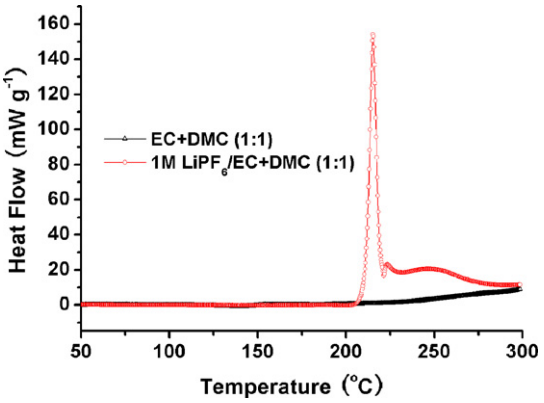


**Fig. 2.** C80 heat flow curves of 1 M $LiPF_6$/EC + DMC electrolyte and EC + DMC solvents at a heating rate of 0.2 °C $min^{-1}$. The mass of sample is 1.0 g.

of C–H bands in the carbonate compounds (EC and DMC). At 30 °C, the peak at 3003 $cm^{-1}$ is related to $CH_2$ groups of EC, and the peaks at 2934 $cm^{-1}$ and 2852 $cm^{-1}$ belong to the $CH_3$ groups of DMC. The three signals have not changed when the temperature rises to 90 °C, which suggests that the carbonates have not been involved in any reaction. But when the temperature exceeds 150 °C, significant changes appear. The peak at 3003 $cm^{-1}$ weakens gradually and vanishes at 220 °C along with a new signal at 2958 $cm^{-1}$ appears and becomes gradually stronger, which may be attributed to the ring-opening polymerization of EC [31]. At the temperature range of 150–250 °C, there is no obvious change of the signals at 2925 $cm^{-1}$ and 2852 $cm^{-1}$. At 300 °C, the signals at 2958 $cm^{-1}$, 2925 $cm^{-1}$ and 2852 $cm^{-1}$ weaken obviously compared with the spectrum at 250 °C, and a new signal at 2800 $cm^{-1}$ appears. As for the spectra in the range of 1000–1900 $cm^{-1}$, there is also no obvious difference between the signals at 30 °C and at 90 °C, but the whole intensity of the spectra is decreased at elevated temperatures above 90 °C mainly because some reaction products reduce the transparency of the sample cell at above 150 °C and perhaps DMC with a boiling point of 90 °C partly escapes from the sample cell without high pressure-proof performance. Around 1800 $cm^{-1}$, the strong peaks originate from the typical stretching mode of carbonyl groups of carbonates. At 150 °C, the signals at 1800 $cm^{-1}$ and 1770 $cm^{-1}$ obviously weaken but the signal at 1850 $cm^{-1}$ still keeps intensive. The change of those signals compared with at 90 °C, is attributed to the ring-opening polymerization of EC, and the weakened signals at 1000–1200 $cm^{-1}$ corresponding to the ring structure of EC also indicate that the ring-opening reaction has occurred, which is consistent with the change of signals at 3003 $cm^{-1}$. When the temperature increases from 150 °C to 250 °C, especially from 220 °C to 250 °C, the peak at 1820 $cm^{-1}$ weakens and eventually vanishes, which suggests that the carbonate group (—O—C(=O)—O—) has undergone a decomposition reaction with $CO_2$ released. Thus, based on all the spectra at different temperatures, it can be concluded that below 220 °C the main reaction is the ring-opening reaction of EC, while the carbonate group (—O—C(=O)—O—) decomposes and releases $CO_2$ above 220 °C. The in-situ FTIR spectra of the solvent of EC + DMC heated to different temperatures are shown in Fig. 1b, in order to investigate the role of $LiPF_6$ in the ring-opening reaction of EC. Below 250 °C, the spectra have no special change with temperature elevated, which indicates that the ring-opening reaction of EC would not occur without $LiPF_6$.

Fig. 2 shows the heat flow curves of 1 g electrolyte of 1 M $LiPF_6$/EC + DMC and 1 g solvent of EC + DMC measured from the C80 calorimetry. The onset temperature of the electrolyte is about 202 °C, and a strong exothermic peak appears at 215 °C, which means that some reactions have been induced around this temperature. After about 225 °C, a mild exothermic process takes place in a wide temperature range with a relatively lower heat flow. Here we believe that the former process (before 225 °C) with the stronger heat generation corresponding to the exothermic reactions is the major factor for thermal stability of Li-ion batteries compared with the latter process, from the standpoint of electrolyte. After the calorimetry measurement, the C80 sample cell was opened and quite a little black solid residua were found. The FTIR spectra of the residua (not shown here) is found basically consistent with the spectra at 300 °C (in Fig. 1a). As the calorimetric study is combined with the results of in-situ FTIR spectra, we agree with the similar reaction mechanism proposed by Sloop [31]. The catastrophic reactions probably include the open-ring polymerization of EC that usually produces rather large reaction heat in a short period. And after 225 °C, the products obtained earlier undergo a series of decomposition with heat generated slowly. Compared with the electrolyte, the solvent of EC + DMC has negligible heat flow, especially below 250 °C, which is also consistent with the in-situ FTIR results (Fig. 1b).

Based on the studies about the thermal reaction mechanism of electrolyte, effect of several cathode materials on the thermal characteristic of the electrolyte has been investigated by C80 calorimtery. The cathode materials have been divided into three categories: cobalt-based metal oxides ($LiCoO_2$, $LiNi_{0.8}Co_{0.15}Al_{0.05}O_2$, $LiNi_{1/3}Co_{1/3}Mn_{1/3}O_2$) (Fig. 3a), manganese-based metal oxides ($LiMn_2O_4$, $LiNi_{0.5}Mn_{0.5}O_2$, $LiNi_{0.5}Mn_{1.5}O_4$, $LiNi_{1/3}Co_{1/3}Mn_{1/3}O_2$) (Fig. 3b) and olivine phosphate ($LiFePO_4$) (Fig. 3c). All of these cathode materials are used for C80 calorimetry after they have been charged to a certain state. At the charge state, $LiCoO_2$ is transformed to $Li_{0.5}CoO_2$, $LiNi_{0.8}Co_{0.15}Al_{0.05}O_2$ to $Li_{0.33}Ni_{0.8}Co_{0.15}Al_{0.05}O_2$, $LiNi_{1/3}Co_{1/3}Mn_{1/3}O_2$ to $Li_{0.3}Ni_{1/3}Co_{1/3}Mn_{1/3}O_2$, $LiMn_2O_4$ to $Li_0Mn_2O_4$, $LiNi_{0.5}Mn_{0.5}O_2$ to $Li_{0.33}Ni_{0.5}Mn_{0.5}O_2$, $LiNi_{0.5}Mn_{1.5}O_4$ to $Li_0Ni_{0.5}Mn_{1.5}O_4$, and $LiFePO_4$ to $Li_0FePO_4$. All of the lithium contents are calculated based on their respective discharge capacity. The ratio between the mass of the electrolyte and cathode in the C80 test is controlled at about 2:1, which is much higher than that in commercial Li-ion batteries. However, the higher mass ratio between electrolyte and cathode was recommended by Aurbach and co-workers [32] to investigate the interaction between the transition metal ions dissolved from the cathodes and the electrolyte. And we also find that a cathode solid sample alone shows much less thermal effect than pure electrolyte below 225 °C (Fig. 4) [33,34], which is also validated by the Dahn's work [20,35] and the Amine's work [36]. Here more attention was focused on the effect of various cathode materials on the thermal stability of electrolyte. Consequently, despite the fact that the electrolyte/cathode ratio herein is high compared with practical systems, the results presented in Fig. 3 are still meaningful.

Fig. 3a shows the heat flow curves of the Co-based cathode materials with the electrolyte, from which the boundary of 225 °C exists distinctly as in the case of the electrolyte alone (Fig. 4). Compared with the electrolyte, the coexisting systems of cathode and electrolyte exhibit lower onset temperatures of exothermic peaks. For LCO and L333, the main exothermic peaks appear at the same position of about 215 °C, which is consistent with that of the electrolyte alone. What is different from the electrolyte alone is the small exothermic peak before the main peak when the cathode materials are introduced, which perhaps is the result of decomposition of the cathodes. As for the cathode material of Gen2, the main exothermic peak is at 198 °C, much lower than that (215 °C) for the electrolyte, together with a relatively small peak appearing at 210 °C. We believe that some violent reactions between the Gen2 cathode and the electrolyte should be responsible for it, or that oxygen liberated from the cathode results in the combustion reaction of the electrolyte [37]. After 225 °C, there is another exothermic peak for all of the three systems, among which, the systems con-

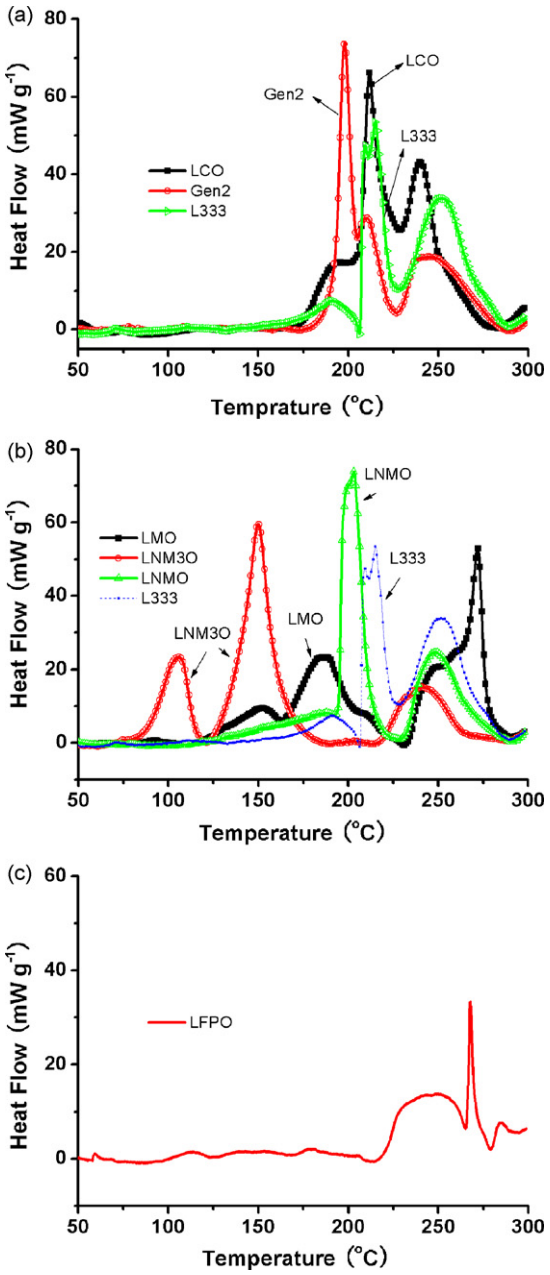


**Fig. 3.** C80 heat flow curves of coexistence systems of 50 mg electrolyte (1 M $LiPF_6$/EC + DMC) and 23 mg delithiated cathode materials at a heating rate of 0.2 °C $min^{-1}$. (a) Co-based cathode materials containing LCO (cut-off at 4.2 V), Gen2 (cut-off at 4.5 V) and L333 (cut-off at 4.5 V), (b) Mn-based cathode materials containing LMO (cut-off at 4.3 V), LNMO (cut-off at 4.5 V), LNM3O (cut-off at 5.0 V) and L333 (cut-off at 4.5 V) and (c) olivine phosphate LFPO (cut-off at 4.2 V).

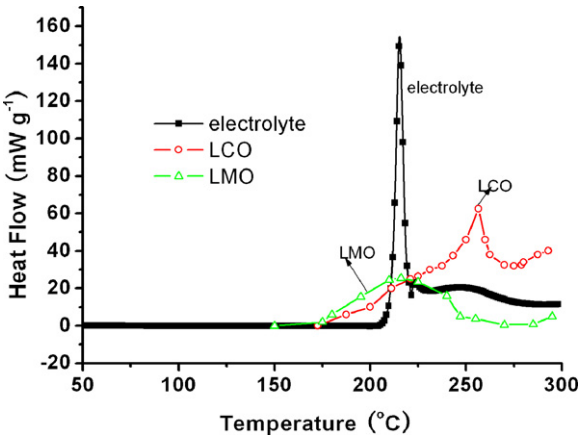


**Fig. 4.** C80 heat flow curves of 1 M $LiPF_6$/EC + DMC electrolyte, LCO (cut-off at 4.2 V, [33]) and LMO (cut-off at 4.3 V, [34]) at a heating rate of 0.2 °C $min^{-1}$. The values of heat flow for LCO and LMO were evaluated from the sample weight of LCO and LMO.

taining Gen2 and L333 have lower heat flow values than that of LCO.

Fig. 3b shows the heat flow curves of the Mn-based cathode materials with the electrolyte. It can be found easily that their onset temperatures are usually lower than those for the systems containing the Co-based cathode materials, which may be because Mn ion is more severely dissolved in the electrolyte than Co ion, especially for materials with the spinel structure (LMO and LNM3O). The first peak temperatures of the spinel cathodes of LMO and LNM3O are 152 °C and 106 °C, respectively. Two distinct exothermic processes for the spinel Mn-based cathode systems appear below the 225 °C, and the temperatures of peaks are quite lower than that of the corresponding peak of pure electrolyte. Different from the two Mn-based cathodes mentioned above, LNMO with the layered structure gives rise to a specially strong exothermic peak around 200 °C along with a negligible exothermic process before, similar as the system of L333. The exothermic peak at 200 °C is believed to be associated with the similar effect of Gen2 on the electrolyte decomposition with the 198 °C exothermic peak. Among the Mn-based cathodes, LMO shows always the relatively lower heat flow before 225 °C, which is mainly because no oxygen released at the lower temperature (<225 °C) induces combustion reaction of electrolyte, although many other reactions have taken place with a relative moderate grade.

Fig. 3c shows the heat flow curve of olivine phosphate cathode material, LFPO, with the electrolyte. Obviously, there is a negligible heat released below 225 °C for the LFPO system, and the onset temperature of significant heat generation is 218 °C. During the whole testing process, the heat flow always keeps at a low level. Based on the thermal characteristic of pure electrolyte, LFPO seemingly has a suppressive effect on the decomposition of electrolyte, which can also be concluded from the ARC results of and Jiang and Dahn's work

**Table 1**
Details on C80 results of the $LiPF_6$-based electrolyte with or without seven cathode materials. The sign "*" shows the maximal exothermic peak. All calculations are based on the weight of the electrolyte.

| Cathode | Upper cut-off voltage (V) | Onset temperature (°C) | Exothermic peak (°C) | | | Reaction heat (J $g^{-1}$) | |
|---|---|---|---|---|---|---|---|
| | | | | | | 50–225 °C | 50–300 °C |
| Electrolyte | – | 202 | 215* | | | 258 | 612 |
| LCO | 4.2 | 168 | 193 | 212* | 240 | 358 | 692 |
| Gen2 | 4.5 | 176 | 198* | 210 | 244 | 318 | 522 |
| L333 | 4.5 | 146 | 191 | 215* | 252 | 255 | 600 |
| LMO | 4.3 | 110 | 152 | 186 | 248, 272* | 308 | 638 |
| LNMO | 4.5 | 115 | 202* | 248 | | 378 | 595 |
| LNM3O | 5.0 | 78 | 106 | 150* | 240 | 485 | 630 |
| LFPO | 4.2 | 218 | 246 | 268* | 285 | 35 | 260 |

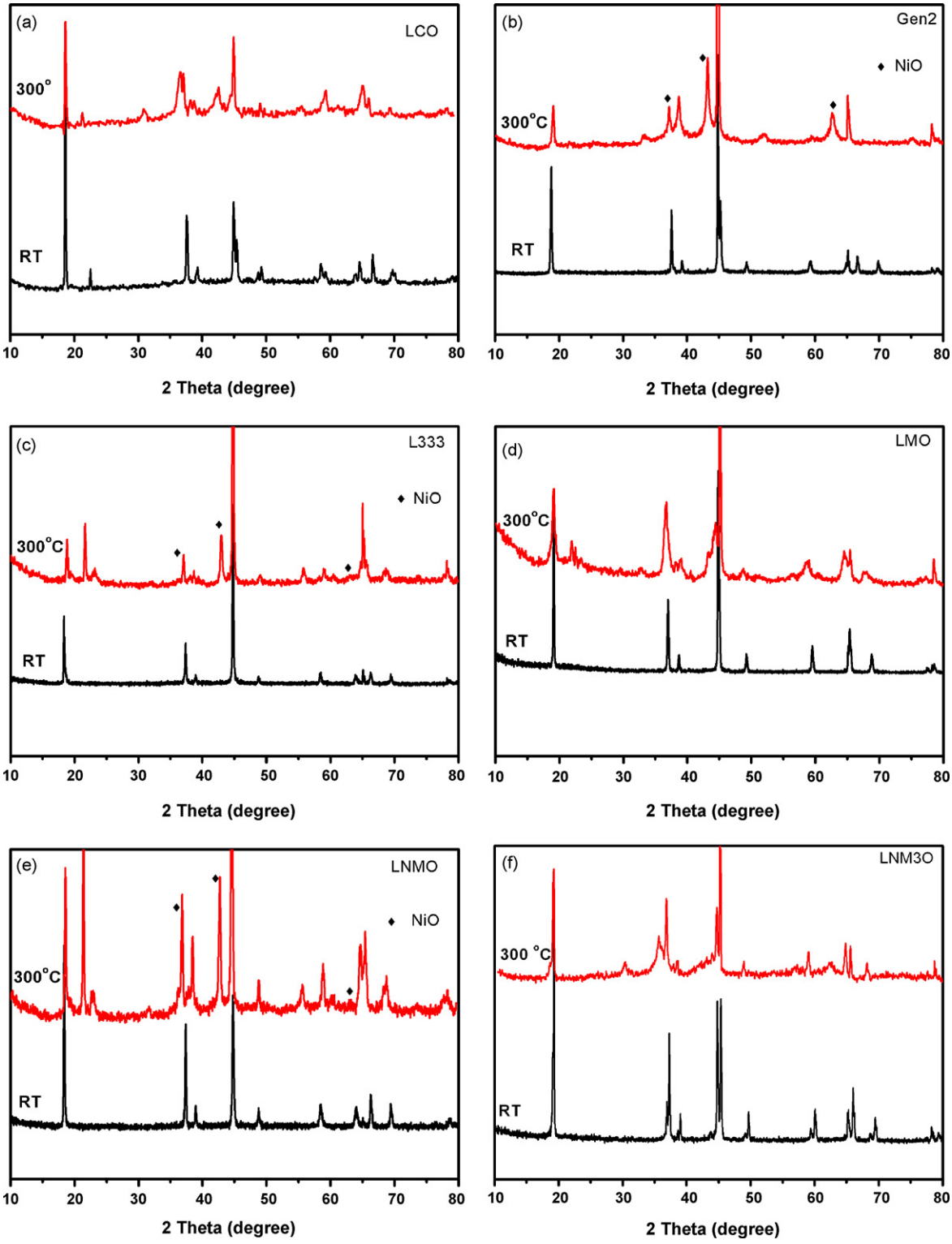


**Fig. 5.** XRD patterns of various cathodes at room temperature and heated to 300 °C. (a) LCO, (b) Gen2, (c) L333, (d) LMO, (e) LNMO, (f) LNM3O and (g) LFPO.

[35]. In that reference paper, the mixture of 100 mg fully delithiated state ($FePO_4$) and 100 mg electrolyte of 1 M $LiPF_6$/EC + DEC electrolyte usually had much lower self-heating rate than 100 mg electrolyte alone at the same temperature, despite the fact that the former had a lower onset temperature. We surmise that some active groups (e.g. unsaturated $PO_4^{3-}$) on the surface of LFPO would capture the Lewis acid $PF_5$ in the electrolyte, while $PF_5$ is widely considered as a catalyst of the decomposition reaction of the electrolyte [31]. The exact reason for the suppressive effect of LFPO on the exothermic reactions of $LiPF_6$-based electrolyte is beyond the range of this paper and should be a subject of further study.

Details on C80 results of electrolyte with or without seven cathode materials are compared in Table 1. Here two indicators, we think, are closely related to the possibility of thermal runaway of a lithium-ion battery. One is the reaction heat released before 225 °C, which is affected directly by reactions between the cathode

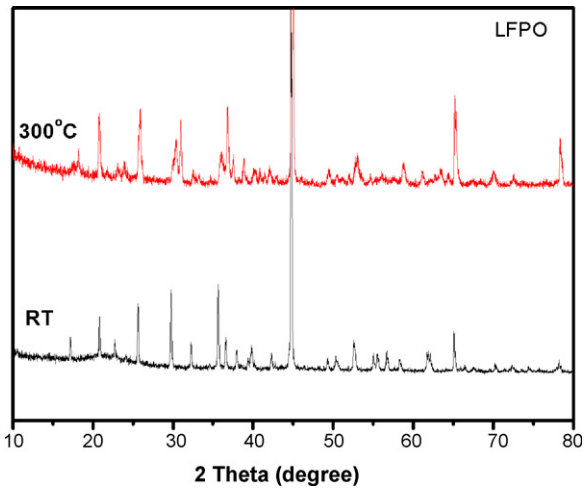


**Fig. 5.** (*Continued*).

used and electrolyte. The thermal runaway of the battery mostly occurs below 200 °C, so it is less important to discuss the reaction heat at higher temperature (>225 °C). Since the main reaction of electrolyte and effect of cathode are reflected at this range of temperature (<225 °C) based on the C80 results above, the reaction heat released before 225 °C is considered as one of the most important indicator for evaluating the thermal stability of Li-ion batteries. The other important indicator is the maximal heat flow. Since thermal runaway appears when the heat generation surpasses the heat dissipation which is decided by the structure of batteries, the heat collected during the maximal heat flow would be the biggest challenge for exceeding heat dissipation that may turn into the battery runaway. Hence, the battery with lower heat flow is considered to be safer. Besides the two indicators mentioned above, the onset temperature of total heat generation and the temperatures corresponding to exothermal peaks also have very important effect on the thermal stability of Li-ion batteries. Among seven cathode materials investigated in this study, there is no doubt that LFPO is the optimal choice for the safety characteristic of Li-ion batteries, owing to its suppressive effect on the decomposition of electrolyte. On the other hand, the L333 system has the lower reaction heat of 255 J/g during the appointed range of temperature (50–225 °C), equal to the reaction heat of the electrolyte alone, which indicates that L333 has good thermal stability and decomposition reactions with oxygen released do not appear below 225 °C. Thus L333 is also considered as a promising cathode for Li-ion batteries with improved safety characteristic. The LMO system exhibits quite lower heat flow before 225 °C and the maximal heat flow is just one third of that of the L333 system. Thus, LMO is also considered to be quite safe, even though the onset temperature of the LMO system is quite low (110 °C). Furthermore, it can be found easily that Mn-based cathode systems have the lower onset temperature, which is perhaps attributed to the higher solubility of Mn ion in the electrolyte, and 5 V cathode material LNM3O has the worst thermal stability.

In order to investigate the structure change of the cathode materials after the C80 calorimetry, the XRD patterns of the cathodes at room temperature and heated to 300 °C, are parallelized in Fig. 5. Here the reaction mechanisms between cathodes and electrolyte are not discussed in detail, and instead the structure stability of cathode materials in the presence of electrolyte at elevated temperature is our major concern. Some new phases are always produced after the reaction between cathode materials and electrolyte at elevated temperature, along with the structure change of the original cathode materials. Compared with other cathode materials, LCO and LMO have more obvious structure change that the original peaks become weaker and broader after the high temperature reactions. As for L333, Gen2 and LNMO, their original patterns keep sharp and robust, though many new phases appear, which is likely because NiO phase is formed on the surface of cathode materials with oxygen released, but the bulk still keeps stable [36,37]. Therefore, for those materials, their surface area would have significant effect on their thermal stability. And LNM3O we synthesized by RPG method with high surface area shows very bad thermal stability and more new phases seemingly appear (Fig. 5f). However, LFPO with high surface area, which is usually present as the agglomerates of nanometer particles, still keeps excellent thermal stability and the structure only has tiny change in the electrolyte with temperature rising to 300 °C.

## 4. Conclusions

Thermal stability of commercial $LiPF_6$-based electrolyte is first investigated by in-situ FTIR spectroscopy along with C80 calorimetry. Strong exothermic reactions in the $LiPF_6$-based electrolyte happen below 225 °C, which is mainly related to the ring-opening reactions of EC and decomposition of polymeric products. The nature of the cathode material has a major impact on the decomposition of electrolyte, which is embodied below 225 °C. LCO, Gen2, LNMO and LNM3O can release oxygen at elevated temperature and further induce the combustion reaction of $LiPF_6$-based electrolyte. Among the cathode materials mentioned, LNM3O has the worst thermal stability, with the much lower onset temperature and more heat generation below 225 °C. Nevertheless, the reactivity between LMO and electrolyte is more moderate with the lower heat flow, and L333 also has good thermal characteristic with the lower reaction heat below 225 °C. Above all, LFPO has excellent thermal stability against $LiPF_6$-based electrolyte, and it can inhibit the decomposition of electrolyte and has experienced tiny structure change after being heated to 300 °C.

## Acknowledgement

This study was supported by Education Department of Anhui Province (grant no. KJ2009A142).

## References

[1] X.M. Wang, E. Yasukawa, S. Kasuya, J. Electrochem. Soc. 148 (2001) A1058.
[2] X.M. Wang, C. Yamada, H. Naito, G. Segami, K. Kibe, J. Electrochem. Soc. 153 (2006) A135.
[3] K. Xu, M.S. Ding, S. Zhang, J.L. Allen, T.R. Jow, J. Electrochem. Soc. 149 (2002) A622.
[4] Y.E. Hyung, D.R. Vissers, K. Amine, J. Power Source 119–121 (2003) 383.
[5] S. Zhang, K. Xu, T.R. Jow, J. Power Source 113 (2003) 166.
[6] X.L. Yao, S. Xie, C.H. Chen, Q.S. Wang, J.H. Sun, Y.L. Li, S.X. Lu, J. Power Sources 144 (2005) 170.
[7] H.F. Xiang, H.Y. Xu, Z.Z. Wang, C.H. Chen, J. Power Sources 173 (2007) 562.
[8] H.F. Xiang, Q.Y. Jin, C.H. Chen, X.W. Ge, S. Guo, J.H. Sun, J. Power Sources 174 (2007) 335.
[9] H. Sakaebe, H. Matsumoto, Electrochem. Commun 5 (2003) 594.
[10] P.C. Howlett, D.R. MacFarlane, A.F. Hollenkamp, Electrochem. Solid-State Lett. 7 (2004) 97.
[11] J. Xu, J. Yang, Y. NuLi, J. Wang, Z. Zhang, J. Power Sources 160 (2006) 621.
[12] E. Zinigrad, L. Larush-Asraf, J.S. Gnanaraj, H.E. Gottlieb, M. Sprecher, D. Aurbach, J. Power Sources 146 (2005) 176.
[13] M. Egashira, H. Todo, N. Yoshimoto, M. Morita, J.-I. Yamaki, J. Power Sources 174 (2007) 560.
[14] A. Fernicola, F. Croce, B. Scrosati, T. Watanabe, H. Ohno, J. Power Sources 174 (2007) 342.
[15] A. Guerfi, S. Duchesne, Y. Kobayashi, A. Vijha, K. Zaghib, J. Power Sources 175 (2008) 866.
[16] H. Maleki, G. Deng, A. Anani, J. Howard, J. Electrochem. Soc. 146 (1999) 3224.
[17] N. Katayama, T. Kawamura, Y. Baba, J.-I. Yamaki, J. Power Sources 109 (2002) 321.
[18] C.L. Campion, W. Li, B. Lucht, J. Electrochem. Soc. 152 (2005) A2327.
[19] D.D. MacNeil, J.R. Dahn, J. Phys. Chem. A 105 (2001) 4430.
[20] D.D. MacNeil, J.R. Dahn, J. Electrochem. Soc. 148 (2001) A1205.

[21] D.D. MacNeil, J.R. Dahn, J. Electrochem. Soc. 148 (2001) A1211.
[22] Y. Baba, S. Okada, J.-I. Yamaki, Solid State Ionics 148 (2002) 311.
[23] J. Jiang, J.R. Dahn, Electrochem. Commun. 6 (2004) 39.
[24] Y.D. Wang, J.W. Jiang, J.R. Dahn, Electrochem. Commun. 9 (2007) 2534.
[25] I. Belharouak, W. Lu, J. Liu, D. Vissers, K. Amine, J. Power Sources 174 (2007) 905.
[26] J.H. Sun, X.R. Li, K. Hasegawa, G.X. Liao, J. Therm. Anal. Calorim. 76 (2004) 883.
[27] P. Lv, Z. Wang, K. Hu, W. Fan, Polym. Degrad. Stab. 90 (2005) 523.
[28] H. Zheng, D. Hua, R. Bai, K. Hu, L. An, C. Pan, J. Polym. Sci. Part A: Polym. Chem. 45 (2007) 2609.
[29] H.Y. Xu, S. Xie, N. Ding, B.L. Liu, Y. Shang, C.H. Chen, Electrochim. Acta 51 (2006) 4352.
[30] H.F. Xiang, Q.Y. Jin, R. Wang, C.H. Chen, X.W. Ge, J. Power Sources 179 (2008) 351.
[31] S.E. Sloop, J.B. Kerr, K. Kinoshita, J. Power Sources 119–121 (2003) 330.
[32] M. Koltypin, D. Aurbach, L. Nazar, B. Ellis, Electrochem. Solid-State Lett. 10 (2) (2007) A40.
[33] Q.S. Wang, J.H. Sun, X.L. Yao, C.H. Chen, Thermochim. Acta 437 (2005) 12.
[34] Q.S. Wang, J.H. Sun, C.H. Chen, J. Electrochem. Soc. 154 (2007) A263.
[35] J. Jiang, J.R. Dahn, Electrochem. Commun. 6 (2004) 724.
[36] I. Belharouak, W. Lu, D. Vissers, K. Amine, Electrochem. Commun. 8 (2006) 329.
[37] H.J. Bang, H. Joachin, H. Yang, K. Amine, J. Prakash, J. Electrochem. Soc. 153 (2006) A731.